

- ⁸A. M. Polyakov, Phys. Lett. **59B**, 79 (1975).
⁹E. Brézin and Zinn-Justin, Phys. Rev. Lett. **36**, 691 (1975).
¹⁰J. L. Cardy, to be published.
¹¹L. Onsager, Phys. Rev. **65**, 117 (1944).
¹²R. Balian and G. Toulouse, Phys. Rev. Lett. **30**, 544 (1973).

- ¹³D. S. McKenzie, Phys. Rep. **27C**, 37 (1976); H. J. Hilhorst, Phys. Rev. B **16**, 1253 (1977).
¹⁴H. Hamber, to be published.
¹⁵M. Ferer, M. A. Moore, and M. Wortis, Phys. Rev. B **4**, 3954 (1971).
¹⁶J. C. Le Gillou and J. Zinn-Justin, Phys. Rev. B **21**, 3976 (1980).

Effective Potential for a Renormalized d -Dimensional $g\varphi^4$ Field Theory in the Limit $g \rightarrow \infty$

Carl M. Bender

Department of Physics, Washington University, St. Louis, Missouri 63130

and

Fred Cooper and G. S. Guralnik^(a)

Theory Division, Los Alamos Scientific Laboratory, Los Alamos, New Mexico 87545

and

Hector Moreno^(b)

Department of Physics, Washington University, St. Louis, Missouri 63130

and

Ralph Roskies

Physics Department, University of Pittsburgh, Pittsburgh, Pennsylvania 15260

and

David H. Sharp

Theory Division, Los Alamos Scientific Laboratory, Los Alamos, New Mexico 87545

(Received 21 April 1980)

The first four coefficients in the effective potential $V_{\text{eff}}(\varphi_R) = \sum_{n=1}^{\infty} V_{2n} \varphi_R^{2n}$ are calculated for a mass- and wave-function-renormalized $g\varphi^4$ field theory in d space-time dimensions in the limit where the unrenormalized coupling $g \rightarrow \infty$ with the renormalized mass M held fixed. The accuracy of these numerical results is verified by exact analytical calculations of the effective potential performed in 0 and 1 space-time dimensions.

PACS numbers: 11.10.Ef, 11.10.Jj, 11.10.Np

In the previous papers¹⁻³ we have formulated a simple procedure for expanding the Green's functions of a $g\varphi^4$ theory in d -dimensional space-time in inverse powers of the bare coupling constant g . In this paper we indicate how such expansions can be mass and wave-function renormalized, and report the results of extensive calculations of the renormalized n -point Green's functions.

The Lagrangian density describing the $g\varphi^4$ theory in Euclidean space is $\mathcal{L} = \frac{1}{2}(\partial\varphi)^2 + \frac{1}{2}m^2\varphi^2 + \frac{1}{4}g\varphi^4$, where m is the bare-mass parameter. To calculate the connected n -point Green's functions $W_n(x_1, \dots, x_n)$ one introduces a source function $J(x)$ in the functional-integral representation

for the vacuum persistence function Z :

$$Z[J] = \int \mathcal{D}\varphi \exp\left\{-\int d^d x [\mathcal{L} + J(x)\varphi(x)]\right\}. \quad (1)$$

We obtain W_n from $Z[J]$ by

$$W_n(x_1, \dots, x_n) = \frac{\delta}{\delta J(x_1)} \cdots \frac{\delta}{\delta J(x_n)} \ln Z[J] \Big|_{J=0}. \quad (2)$$

The Green's functions are renormalized in three steps: First, the wave-function renormalization constant Z_3 is computed from the two-point Green's function by $Z_3^{-1} = [dW_2^{-1}(p^2)/dp^2]_{p^2=0}$. Second, the renormalized mass M is defined by $M^2 = Z_3[W_2^{-1}(p^2)]_{p^2=0}$. Third, the renormalized n -point Green's functions are obtained by multiply-

ing W_n by $Z_3^{n/2}$ and eliminating m in favor of M . This procedure, in which M and Z_3 are defined at $p^2=0$, is an intermediate renormalization scheme.

An important quantity to calculate in this theory

$$\begin{aligned} V_2 &= M^2/2, \quad V_4 = G/24 = -Z_3^2(W_2^{-1})^4 W_4/4!|_{p=0}, \quad V_6 = -Z_3^3(W_2^{-1})^6 [W_6 - 10W_4^2 W_2^{-1}]/6!|_{p=0}, \\ V_8 &= -Z_3^4(W_2^{-1})^8 [W_8 - 56W_6 W_4 W_2^{-1} + 280W_4^3 (W_2^{-1})^2/8!]|_{p=0}, \end{aligned} \quad (3)$$

and so on. Of particular interest to us is G , the renormalized coupling constant, and $\tilde{G} = GM^{d-4}$, the dimensionless renormalized coupling constant. Because we are primarily concerned here with $d < 4$, we do not perform a coupling-constant renormalization of the higher Green's functions.

To obtain numerical values for the dimensionless quantities $R_{2n} = V_{2n}/M^{2n-n d+a}$, we expand the functional-integral representation for $Z[J]$ on a lattice in powers of g^{-1} . This procedure begins by formally eliminating the kinetic energy term from the functional integral by means of a functional differential operator:

$$Z[J] = \exp \left[\iint d^d x d^d y \frac{1}{2} \frac{\delta}{\delta J(x)} G_0^{-1}(x, y) \frac{\delta}{\delta J(y)} \right] \int \mathcal{D}\varphi \exp \left[- \int d^d x \left(\frac{1}{2} m^2 \varphi^2 + \frac{1}{4} g \varphi^4 + J\varphi \right) \right], \quad (4)$$

where $G_0^{-1}(x, y) = \partial^2 \delta(x - y)$. The remaining functional integral in (4) is evaluated explicitly by expressing it as a product of ordinary integrals, one for each lattice point; each such integral has the form $\int_{-\infty}^{\infty} dx \exp[-a^d (\frac{1}{4} g x^4 + \frac{1}{2} m^2 x^2 + Jx)]$, where a is the lattice spacing.

We asymptotically expand this integral for large g , using two distinct procedures. The first method begins by holding m fixed. The second method is more refined and gives better results. It assumes that in the limit of large g , with M fixed, m^2 becomes large and negative in the continuum theory. One way to incorporate this behavior is to substitute $m^2 = -g\mu^{d-2}$, where μ is regarded as a fixed mass. (There are, of course, many other substitutions which allow m^2 to be large and negative.) In either method, asymptotically expanding the integral for large g , with m fixed in the first case or with μ fixed in the second case, defines a set of $2n$ -point vertices to be used in the diagrammatic expansion of the Green's functions. We have calculated W_2 , W_4 , W_6 , and W_8 up to diagrams having four, five, six, and seven internal lines, respectively, using the vertices obtained by both methods. The resulting calculation gives the Green's functions as double power series in the small dimensionless parameters $\epsilon = (ga^{4-d})^{-1/2}$, $s = m^2 a^2$ (method 1) and $t = (\mu a)^{d-2}$, $x = a^{-4} \mu^{4-2d}/g$ (method 2). The dependence upon the space-time dimension parameter d is very simple; the value of a diagram having k internal lines depends on d as a k th-degree polynomial. The details of these diagrammatic expansions will be given elsewhere.

is the renormalized effective potential $V_{\text{eff}}(\varphi_R) = \sum_{n=1}^{\infty} V_{2n} \varphi_R^{2n}$, where $\varphi_R = Z_3^{-1/2} \varphi_{\text{classical}}$. Since V_{eff} is the generating function of the one-particle-irreducible renormalized Green's functions at zero external momentum on all legs, the coefficients V_{2n} can be expressed as follows:

The renormalization of the n -point Green's functions was carried out by solving for m (or μ) in terms of M . Since M was calculated in the form of a series in powers of the two small parameters (ϵ, s) or (t, x), the resulting expression for M is itself a series in powers of these small parameters. Upon eliminating m (or μ) in the series for the Green's functions, the parameter s in method 1 gets replaced by $S = M^2 a^2$ and the parameter t in method 2 gets replaced by $T = 1/M^2 a^2$. Here we are interested in the limits $a \rightarrow 0$, $g \rightarrow \infty$, with M fixed, and so we set S and x to zero.⁴ Thus, the remaining parameters are ϵ (method 1) and T (method 2), and the truncated series in powers of these parameters must be extrapolated to infinite values of ϵ and T .

The procedure we use to extrapolate to the continuum limit ($\epsilon \rightarrow \infty$, $T \rightarrow \infty$) has been extensively described and investigated.^{2,3} Typically, the procedure yields a sequence of extrapolants, one for each order of perturbation theory (in powers of ϵ or T in this case) which appear to converge rapidly to limits. These limits are presumably the correct answers for the continuum theory. In Table I five extrapolants to \tilde{G} for several values of d are given. Observe that the extrapolants to \tilde{G} from method 2 are far more rapidly convergent than those obtained from method 1. On the basis of Table I we select method 2 as the superior method; all further numerical results reported here are derived using method 2.

There are a number of techniques which can be used to extrapolate to $T = \infty$. One such technique,

TABLE I. Five extrapolants to \tilde{G} from method 1 and method 2. Observe that the extrapolants from method 2 converge more rapidly as might be expected because method 2 incorporates the fact that m^2 is large and negative for large g . The inadequacy of method 1 is particularly apparent in three dimensions because it predicts complex values for \tilde{G} . The exact result for \tilde{G} when $d=1$ is 6 [see (7)].

Number of internal lines	$d=1$		$d=2$		$d=3$	
	Method 1	Method 2	Method 1	Method 2	Method 1	Method 2
2	4.086	5.657	12.381	16.000	62.526	45.255
3	4.526	5.826	10.555	14.966	complex	31.811
4	4.970	5.895	12.580	14.930	30.498	30.984
5	5.178	5.931	14.283	14.986	complex	30.149
6	5.354	5.952	15.703	14.945	49.012	28.426

which leads to the results in Table I, is to extrapolate the series in powers of T directly. An alternative suggested by Baker is to map the parameter T ($0 \leq T \leq \infty$) into a new parameter Q ($0 \leq Q \leq 1$) by the transformation $T = Q/[(1-Q)(2d+2)]$. After making this substitution, reexpanding the series in powers of Q , converting the resulting series into Padé form, and evaluating the Padé approximants at $Q=1$ we obtain a new sequence of extrapolants. We have found strong agreement between T extrapolants and Q extrapolants for $d < 3.5$ giving us confidence in our numerical results.

Figure 1 is a graph of the 4th-, 5th-, and 6th-order T extrapolants for \tilde{G} as a function of d for $0 \leq d \leq 4$. A striking feature of this graph is that the approximants to \tilde{G} , $d \geq 2$, are decreasing as the order of perturbation theory increases, and

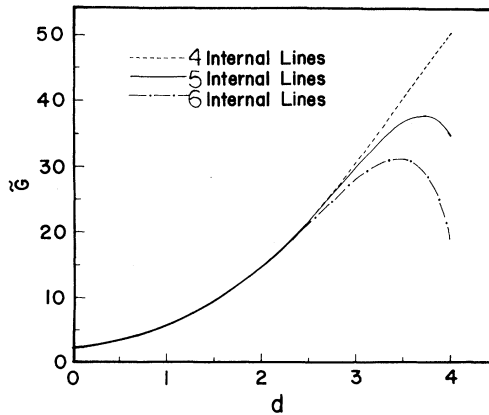


FIG. 1. A plot of the T extrapolants to \tilde{G} for $0 \leq d \leq 4$ from diagrams having up to four, five, and six internal lines. Note that the approximants to \tilde{G} decrease with increasing order of perturbation theory when $d > 2$.

may even be tending to zero. For $d=4$ such behavior has also been observed by Kogut and Wilson⁵ and by Baker and Kincaid.⁶ In Fig. 2 we give our last extrapolant to the values of the dimensionless effective-potential coefficients R_6 and R_8 and observe a similar trend.⁷

Some of the results in Fig. 2 are verified by exact calculations which will be reported in detail elsewhere. These calculations are based on the idea that in the limit $g \rightarrow \infty$, with M fixed, the functional integral in (2) is dominated by instantons, at least for small values of d . Polyakov⁸ and Gildener and Patrascioiu⁹ have shown how to calculate the two-point function in one-dimensional space-time using the dilute-instanton-gas ap-

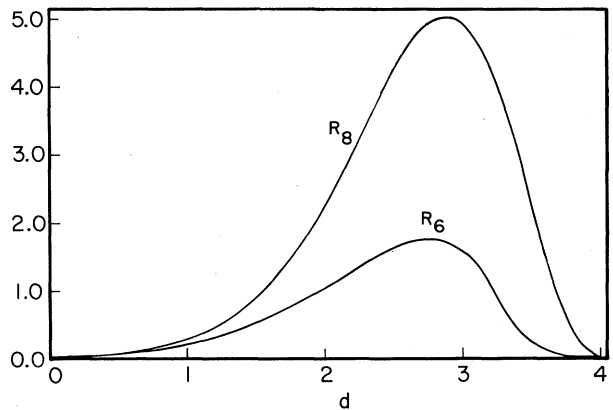


FIG. 2. Last extrapolant for the dimensionless effective-potential coefficients R_6 and R_8 . Note that the extrapolants at first increase and then decrease thus exhibiting the same behavior as the extrapolants to \tilde{G} in Fig. 1 and Table I. The exact values are $\frac{1}{30}$ ($d=0$) and $\frac{1}{4}$ ($d=1$), and $\frac{1}{56}$ ($d=0$) and $\frac{1}{16}$ ($d=1$) for R_6 and R_8 , respectively [see (7)].

proximation. Their calculations, which are lengthy and difficult, give the result that $W_2(x, y) = \frac{1}{2}A \exp(-M|x-y|)$, where A is a calculable constant. However, the general form of W_2 can be easily derived. One assumes that in the instanton limit the anharmonic oscillator potential

$$W_2(x-y) = \langle 0 | T[\varphi(x)\varphi(y)] | 0 \rangle = \sum_n |\langle 0 | \varphi(0) | n \rangle|^2 \exp[-(E_n - E_0)|x-y|] \simeq |\langle 0 | \varphi(0) | 1 \rangle|^2 \exp(-M|x-y|). \quad (5)$$

By a similar argument, we conclude that the higher Green's functions factor into a product of two-point functions:

$$\langle 0 | \varphi(x_1)\varphi(x_2) \cdots \varphi(x_{2n}) | 0 \rangle \simeq \langle 0 | \varphi(x_1)\varphi(x_2) | 0 \rangle \cdots \langle 0 | \varphi(x_{2n-1})\varphi(x_{2n}) | 0 \rangle, \quad (6)$$

in which the order of the x 's is preserved. The results in (5) and (6) allow us to compute the coefficients V_{2n} , with use of (3). It is remarkable that the constant A drops out of the final expression for V_{2n} . Our results are¹⁰

$$V_{2n} = M^{2n} / [2n(2n-1)] \quad (d=0), \quad (7)$$

$$V_{2n} = [M^{n+1} 2^n \Gamma(n - \frac{1}{2})] / [4\Gamma(\frac{1}{2})n!] \quad (d=1).$$

The results in (7) serve as a benchmark for our numerical calculations; they show that the approximants listed in Table I and Fig. 2 for $d=0$ and $d=1$ have an error of a few percent.

Using our techniques we have also calculated the first two correction terms in the series expansion for \tilde{G} in powers of M^{4-d}/g . These terms are negative and vary with d like the curves in Figs. 1 and 2.

We are deeply indebted to George A. Baker for valuable assistance and helpful suggestions on many aspects of this work. We thank the Massachusetts Institute of Technology MATHLAB group for the use of MACSYMA. We thank the National Science Foundation and the U. S. Department of Energy for financial support. We also thank the Brown University Materials Research Lab for partial support under its National Science Foundation grant.

^(a)Permanent address: Physics Department, Brown University, Providence, Rhode Island 02912.

^(b)On leave of absence from Centro de Investigación y de Estudios Avanzados del Instituto Politécnico Nacional, 14-740 México 14, D. F., Mexico.

¹C. M. Bender, F. Cooper, G. S. Guralnik, and D. H.

is an infinitely deep double well. In such a well the two lowest energy levels, E_0 and E_1 , are nearly degenerate ($E_1 - E_0 = M$, the renormalized mass) compared with $E_n - E_0$ ($n \geq 2$); that is ($E_n - E_0$)/ $M \gg 1$. With this assumption, it follows that W_2 has the above form because

Sharp, Phys. Rev. D 19, 1865 (1979).

²C. M. Bender, F. Cooper, G. S. Guralnik, R. Roskies, and D. H. Sharp, Phys. Rev. Lett. 43, 537 (1979).

³C. M. Bender, F. Cooper, G. S. Guralnik, E. Mjolsness, H. A. Rose, and D. H. Sharp, to be published; R. J. Rivers, Phys. Rev. D 20, 3425 (1979).

⁴The lattice theory at $x=0$ is the Ising model; see G. A. Baker, Phys. Rev. B 15, 1552 (1977). When we set $x=0$ our calculations on the lattice agree with those in this reference up to six internal lines.

⁵J. Kogut and K. G. Wilson, Phys. Rep. 12C, 75 (1974).

⁶G. A. Baker and J. M. Kincaid, Phys. Rev. Lett. 42, 1431 (1979); G. A. Baker and J. M. Kincaid, to be published.

⁷To determine whether \tilde{G} is really tending to 0 as the order of perturbation theory increases we fit G on the lattice by $(M^2 a^2)^\gamma$ and determine the value of γ from a Padé calculation. If γ tends to a nonzero constant as the order of perturbation theory increases, then it is safe to conclude that $\tilde{G} \rightarrow 0$. We know that $\tilde{G} = 6$ for $d=1$; for this value of d we compute $\gamma \approx 0.01$. However, when $d=4$, the 4-, 5-, and 6-line approximants to γ are 0.360, 0.333, and 0.324. These approximants decrease and seem to level off at a nonzero value near 0.3. For $d \rightarrow \infty$ we have obtained the exact result that $\gamma/d \sim \frac{1}{2} - 2/d + O(1/d^2)$. G. A. Baker has found numerically that the limit $g \rightarrow \infty$ and $a \rightarrow 0$ do not commute in three dimensions (hyperscaling breaks down). One possible interpretation of these results is that for d sufficiently large one cannot define a nontrivial field theory in which the order of the limits is $g \rightarrow \infty$ first and then $a \rightarrow 0$.

⁸A. M. Polyakov, Nucl. Phys. B120, 429 (1977).

⁹E. Gildener and A. Patrasciouiu, Phys. Rev. D 16, 423 (1977).

¹⁰With use of (7) and summing the series gives closed form expressions for the effective potential: $V_{\text{eff}} = \frac{1}{2}M[(1+x)\ln(1+x) + (1-x)\ln(1-x)]$ ($d=0$) and $V_{\text{eff}} = \frac{1}{2}M[1 - (1-2x^2)^{1/2}]$ ($d=1$), where $x = \varphi_R M^{1-d/2}$.